Predicting χ of polymer blends

using atomistic morphing simulations

Shreya Shetty,[†] Enrique D. Gomez,^{†,‡,¶} and Scott T. Milner^{∗,†,‡}

†Department of Chemical Engineering, The Pennsylvania State University, University
Park, PA, 16802

‡Department of Materials Science and Engineering, The Pennsylvania State University,
University Park, PA, 16802

¶Materials Research Institute, The Pennsylvania State University, University Park, PA,
16802

E-mail: stm9@psu.edu

Abstract

The Flory Huggins interaction parameter χ measures the compatibility of different species in mixtures and governs their phase behavior. We have previously used molecular dynamics (MD) simulations and thermodynamic integration along the path of transformation of one species to another (morphing), to determine χ in coarse-grained bead-spring models of polymer blends. In this work, we use united-atom (UA) MD simulations and morphing to calculate χ for real polymer blends: (1) poly(ethylene) and poly(ethylene oxide), (2) poly(styrene) and poly(2-vinyl pyridine), (3) poly(isoprene) and saturated poly(isoprene) and (4) poly(styrene) and poly(α -methyl styrene). These examples require different schemes for transforming chains: changing Lennard Jones parameters and partial charges (case 1 and 2), transforming double bonds to single bonds (case 3), and making atoms disappear (case 4). For the first three blends, χ

predictions agree reasonably with experiments, but are sensitive to the choice of force field parameters. For $PS/P\alpha MS$, we reach the limits of the morphing method.

Introduction

Polymer blends and block copolymers allow access to material properties unattainable with single component melts. For example, poly(styrene) (PS) is added to poly(phenylene oxide) (PPO) to lower the melting temperature and improve processability. Blending poly(vinylidene fluoride) (PVDF) with poly(methyl methacrylate) (PMMA) improves solvent and UV resistance. Immiscible blends of poly(propylene) (PP) and poly(urethane) (PU) are used commercially in coatings, packing materials, membranes, adhesives, resins, and optoelectronics. Block copolymers provide nano-scale polymer domains, resulting from interactions and connectivity between different components, with increasing applications in microelectronics, membranes, drug delivery, and lithography. In the same provides and statement of the same provides are supplied to the same provides and same prov

The physical properties of polymer blends and block copolymers depend strongly on their morphology.^{8,9} A key factor governing the phase behavior of polymer mixtures is the excess free energy of mixing, quantified by the Flory Huggins interaction parameter χ . It accounts for non-ideal mixing effects caused by differences in monomer size, interactions, and molecular architecture.^{6,10} The design of new materials with desired properties requires a description of how the molecular properties affect χ .

Various experimental methods have been used to measure χ for polymer mixtures. These include melting point depression, ¹¹ heat of mixing, ¹² cloud points, ¹³ osmotic pressure, ¹⁴ and inverse gas chromatography. ¹⁵ X-ray and neutron scattering, in combination with the random phase approximation (RPA), has also been used to extract χ parameters for miscible blends. ^{16,17} For strongly segregated block copolymer mesophases, χ can be obtained by measuring interfacial width, contact angle, and domain spacings. ^{18,19} Note that χ parameters measured using different experimental methods often are inconsistent with each other. ²⁰

Predicting χ of real polymer blends using simulations is challenging. Several computational studies approximate χ , either from cohesive energy densities or by measuring coordination numbers and interaction energies. ^{21,22} Callaway et al. used this method to measure χ of poly(epichlorohydrin) and poly(methyl acrylate) and found that the value for χ matches experiments reasonably well, although experimental values had large variances. ²³ Chen et al. used Gibbs Ensemble Monte Carlo (GEMC) simulations to predict χ for poly(ethylene-alt-polypropylene) (PEP) and poly(ethylene oxide) (PEO) mixtures. They studied the effect of molecular weight and dispersity on χ . ²⁴ This method accounts for enthalpic and entropic contributions to χ . But to increase the acceptance probability for switching chains across different phases, they have implemented advanced sampling techniques, which require extensive coding.

We have developed a method to determine χ that combines molecular dynamics (MD) simulations and thermodynamic integration along a path of transformation of polymer chains from one species to another.^{25–27} The excess free energy of mixing ΔG_{ex} is given by

$$\beta \Delta G_{ex} = \beta G_{AB} - \phi_A \beta G_A - \phi_B \beta G_B \tag{1}$$

Here G_{AB} , G_A , and G_B are free energy of the mixture, homopolymer A, and homopolymer B respectively. ϕ_A and ϕ_B are volume fractions of polymer A and B in the blend. χ can be computed from ΔG_{ex} using

$$\frac{\beta \Delta G_{ex}}{V} = \frac{\phi_A \phi_B \chi}{\nu} \tag{2}$$

Here V is the volume of the system and ν is the reference volume ($\nu = 0.1 \text{ nm}^3$).

To measure ΔG_{ex} , we perform two series of MD simulations in which polymer A chains are transformed into polymer B. We measure G_B and G_{AB} from two simulation series, where we morph all the chains and half of the chains in the system respectively, as thermodynamic work required to morph the chains from A to B. Homopolymer A serves as reference state $(G_A = 0 \text{ in equation } 1)$.

In previous works, we have applied this morphing method to bead-spring chains, to study the effect of different factors on χ . Kozuch et al. first used this method to study the effect of chain backbone stiffness mismatch, with results in agreement with field theory predictions of Fredrickson et al. ^{17,25} Zhang et al. extended this method to study how Lennard-Jones (LJ) interaction mismatch affects χ . ²⁶ The resulting χ values were validated by comparing the interface shape for a phase-separated binary blend predicted by self consistent field theory (SCFT) with MD simulation results. Shetty et al. explored the effects of chain architecture on χ for bead-spring chains with side groups and a differently interacting bead at different locations in the monomers of half the chains. ²⁷

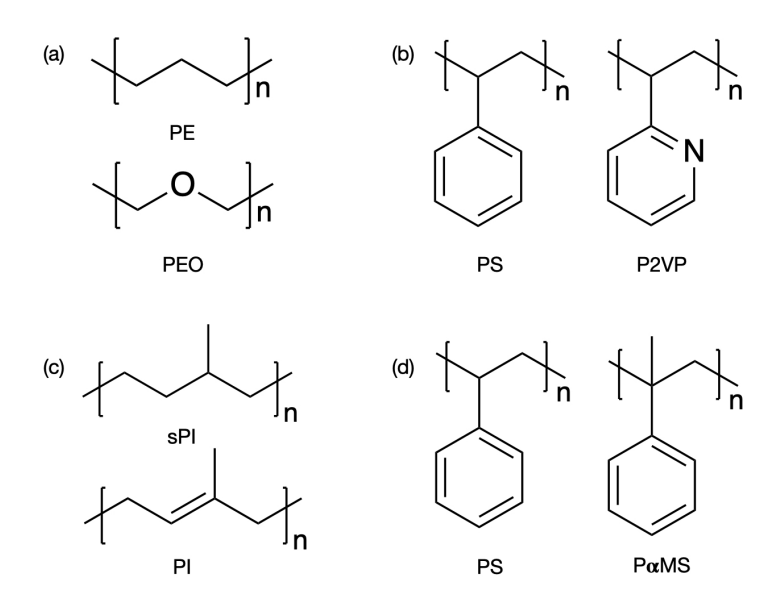


Figure 1: Molecular structure of polymers studied in this work.

In this study, we extend the morphing method to predict χ for real polymer blends (Figure 1): (a) poly(ethylene) / poly(ethylene oxide) (PE/PEO), (b) poly(styrene) / poly(2-vinyl pyridine) (PS/P2VP), (c) poly(isoprene) / saturated poly(isoprene) (PI/sPI) and (d) poly(styrene) / poly(α -methyl styrene) (PS/P α MS). For these four systems, the magnitude of experimental χ values vary from an order of 10^{-1} to 10^{-4} . These four examples require different approaches to morph one species into the other.

We perform a series of united atom MD simulations in which we transform the chains

and measure excess free energy of mixing. Using this method, we predict χ values that agree reasonably with experiments for the first three examples. For PS/P α MS, we are not able to predict a reliable χ , as a very small value of ΔG_{ex} is obtained from the difference between two relatively large quantities G_{AB} and G_{B} . We also explore how χ depends on the value of potential parameters and dielectric constant used in the simulations. Finally, our method allows us to separately compute enthalpic and entropic contributions to χ , which we find are comparable for several of the cases studied, highlighting the importance of computing the free energy and not just the energy.

Methods

Excess free energy from simulations

We use MD simulations and thermodynamic integration along the path defined by a series of simulations to compute χ for a given blend. Consider a blend composed of polymer species A and B. We perform two series of simulations, through which the polymer chains transform from A to B. In the first case, we transform half the chains to create an A/B blend; in the second we transform all the chains to form a pure B melt. We define a parameter λ , called the morphing parameter, to describe how similar the chains are to the final state. The chains transform from A to B through the simulation series and λ changes from 0 to 1.

We measure the work required to transform the polymer chains in the simulations. The work to morph the chains by $\partial \lambda$ at a given λ , $(\partial G/\partial \lambda)_{\lambda}$, is given by

$$\left(\frac{\partial G}{\partial \lambda}\right)_{\lambda} = \frac{\int \int (\partial E/\partial \lambda) \exp\left[\beta E_{\lambda}\right] d\mathbf{r} d\mathbf{q}}{\int \int \exp\left[\beta E_{\lambda}\right] d\mathbf{r} d\mathbf{q}} = \left\langle\frac{\partial E}{\partial \lambda}\right\rangle_{\lambda} \approx \frac{\langle \Delta E\rangle_{\lambda}}{\Delta \lambda} \tag{3}$$

where \mathbf{r} and \mathbf{q} are the position and momentum of atoms in the system. Here we approximate the derivative $\partial E/\partial \lambda$ by a finite difference; $\langle \Delta E \rangle_{\lambda}$ is the change in the system energy for a small change $\Delta \lambda$ at λ . To compute $\langle \Delta E \rangle_{\lambda}$, we rerun the simulation trajectory at a given λ

with interaction parameters associated with adjacent λ values, and measure the total energy of the system for the reruns. $\langle \Delta E \rangle_{\lambda}$ is the difference in the rerun total energies divided by $\Delta \lambda$.

To calculate χ , we calculate the free energy of morphing to blend (G_{AB}) and the free energy of morphing to pure melt of polymer B (G_B) , with polymer A as the initial state $(G_A = 0)$. We integrate $(\partial G/\partial \lambda)_{\lambda}$ with respect to λ to calculate the free energy of morphing. From the simulation series where all the chains in the pure melt of polymer A morph to obtain a pure melt of polymer B, we measure the free energy of morphing to pure melt B, denoted G_B . In the second simulation series, half of the chains in the melt of polymer A morph to obtain a blend of polymer A and B and we measure the free energy of morphing to the blend, G_{AB} . We then calculate the excess free energy of mixing ΔG_{ex} (equation 1) and χ using equation 2.

Simulation details and morphing schemes

In this paper, we extract χ using the morphing method for following real polymer blends: (1) poly(ethylene) / poly(ethylene oxide) (PE/PEO), (2) poly(styrene) / poly(2-vinyl pyridine) (PS/P2VP), (3) poly(isoprene) / saturated poly(isoprene) (PI/sPI) and (4) poly(styrene) / poly(α -methyl styrene) (PS/P α MS) (Figure 1). The four systems require different transformations, and cover a range of experimental χ values. From these examples, we can determine how small a χ value the method can reliably predict.

We represent the polymers with united atom models for computational efficiency. Single particles represent CH_x moieties as well as heteroatoms like nitrogen and oxygen. We adopt TRAPPE-UA potential parameters to describe both non-bonded and bonded interactions. ^{28,29} GROMACS was used to perform the simulations. ³⁰ The velocity rescaling thermostat and Berendsen barostat with time constants 0.2 ps and 1 ps were used to control temperature and pressure.

Morphing simulations start with equilibrated melts, which were built for each polymer

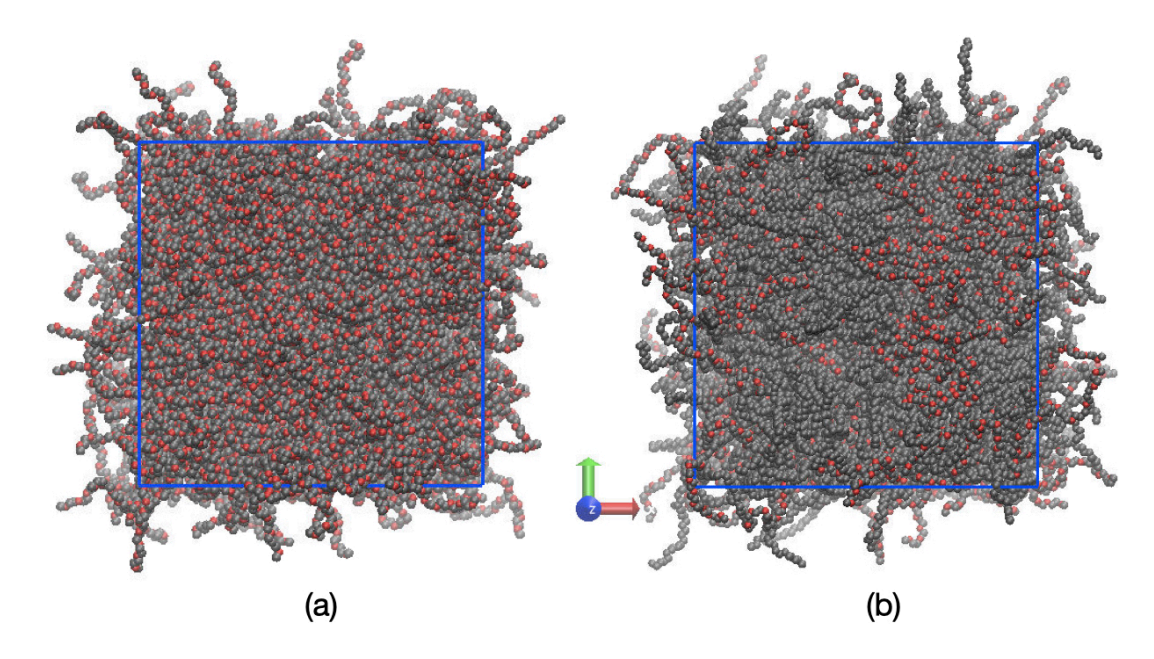


Figure 2: Snapshots of melts obtained after morphing simulations of PE/PEO: (a) pure (PEO); (b) blend (PE/PEO).

blend. Initial configurations were constructed by placing straight polymer chains with ample space between them in a regular array. Atactic chains were built by randomly placing side groups on either side of the chain backbone for all the chains in the system using a Mathematica script. To equilibrate, we minimize the energy, then simulate in an NVT ensemble at T = 500 K for 1 ns. We then simulate while steadily decreasing the volume over 1 ns to reach the equilibrium density. Finally we perform an NPT simulation at T = 500 K and P = 1 bar for 10 ns to obtain an equilibrated melt (See Figure 2).

We morph the chains from one species to another by modifying the potential parameters associated with the transformed atoms. The non-bonded interactions are described by

$$U_{ij}(r) = 4\epsilon_{ij} \left[\left(\frac{\sigma_{ij}}{r_{ij}} \right)^{12} - \left(\frac{\sigma_{ij}}{r_{ij}} \right)^{6} \right] + \frac{1}{4\pi\epsilon_0} \frac{q_i q_j}{r_{ij}}$$
(4)

We modify LJ interactions by varying the interaction parameters ϵ_{ii} and σ_{ii} associated with morphed atoms. Interactions with other atoms are specified by mixing rules, $\epsilon_{ij} = (\epsilon_{ii}\epsilon_{jj})^{1/2}$ and $\sigma_{ij} = (\sigma_{ii} + \sigma_{jj})/2$. Coulomb interactions are morphed by changing the partial charges

on the atom. Bonded interactions involving the morphed atoms are varied by modifying the corresponding potential parameters.

For the four examples presented in this study, the pairs of polymers in the blend have similar molecular structures. Correspondingly, the morphing involves simple changes of nature of atoms, or bonds, or deletion of side group atoms. To implement morphing in simulation series, we override the LJ parameters and bond parameters of involved atoms in "topology" files used in GROMACS with values corresponding to λ associated with given simulation.

PE/PEO

Morphing simulations for PE/PEO blend start with a pure melt of PE chains. We morph one pseudo-atom corresponding to a (CH₂) unit to O in every monomer corresponding to PEO chains. The morph involves the change of LJ interaction parameters and partial charges of all the atoms in the given chain. Bonded interactions involving the morphed pseudo atom are likewise varied. The system consists of 800 chains, with each chain corresponding to 15 monomers of PE. After morphing, a chain becomes 10 monomers of PEO. All simulations were performed at 500 K and 1 bar for 30 ns with a time step of 2 fs.

For comparison, we also perform all-atom (AA) morphing simulations for PE/PEO. In this case, one (CH₂) unit morphs to O in every monomer morphed to PEO, which involves the deletion of hydrogens and changing carbon to oxygen. The system consists of 768 chains of 6-monomer long PE (i.e., $C_{12}H_6$), which morph into 4-monomer PEO chains. (Such short chains were used to speed equilibration). Simulations were performed at 400 K and 1 bar for 30 ns with a time-step of 2 fs. To make an exact comparison between AA morphing simulations and UA morphing simulations, we perform UA morphing simulations with a system with specifications (chain length, temperature) as the ones used in AA simulations.

Chen et al. have used modified TRAPPE force-field parameters to predict χ for polymer blend poly(ethylene-alt-propylene) (PEP) and poly (ethylene oxide) dimethyl ether (PEO)

using GEMC simulations.[?] The parameters were adjusted to match the experimental value for χ . The modified parameters involved smaller partial charges on oxygen (-0.44 e instead of -0.5 e) and neighboring methyl moieties (0.22 e vs 0.35 e), with LJ parameter adjusted to obtain right density for single component melt. We perform UA morphing simulations with these set of modified force-field parameters to compare with results from morphing simulations with original TRAPPE potential parameters.

PS/P2VP

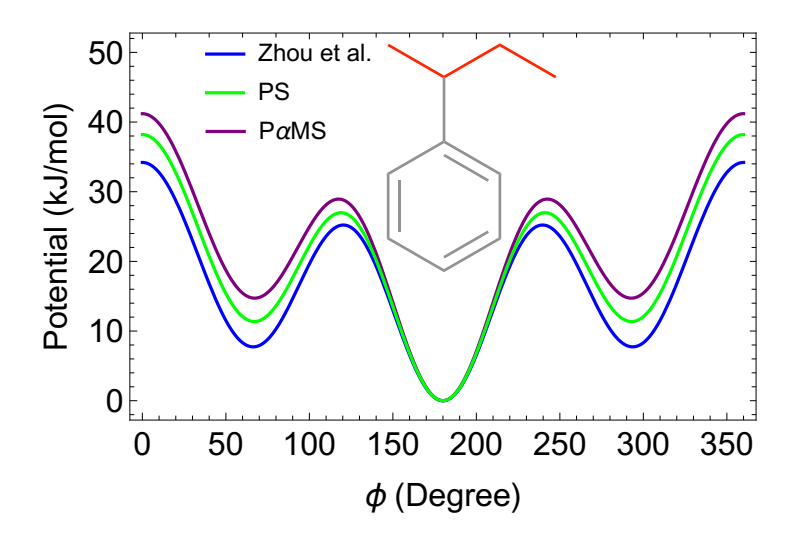


Figure 3: Dihedral potential of the alkyl chain backbone (noted in red in the inset) for PS (green) and P α MS (purple). The blue curve is the dihedral potential used in Zhou et al.³²

Morphing simulations for the PS/P2VP blend start with a pure melt of P2VP chains. We transform P2VP into PS by changing the nitrogen atom in the pyridine ring of P2VP to a CH united atom. We change the LJ parameters and partial charges of the nitrogen atoms, as well as adjacent CH united atoms. Bonded interaction parameters remain the same, as the atom is situated in a rigid aromatic ring.

We find that the dihedral potential parameters for the alkyl chain backbone of PS and P2VP from TRAPPE do not give a persistence length close to experimental values. The dihedral potential for PS used by Zhou et al., which was adjusted to give reasonable local

Table 1: Modified dihedral potential used for PS and P α MS of the form $V(\phi) = \frac{1}{2}[C_1(1 + \cos(\phi)) + C_2(1 - \cos(2\phi)) + C_3(1 + \cos(3\phi)) + C_4(1 - \cos(4\phi))]$. All the constants C_i have units kJ/mol.

	Polymer	C1	C2	C3	C4		
	PS or P2VP	15.54	-1.46	22.66	2.02		
	$P\alpha MS$	18.54	0.04	22.66	2.02		
1.0	,		1.0			4.	
0.8	(;	a)	0.8			(b)	1
₹ 0.6		1	0.6 \$0.4 \$0.4				1
\$\frac{\frac{x}{x}}{2} 0.4		-	\$ 0.4				
0.2			0.2				
			0.0				
0.0	4 6	 8	Ĺ O	2	4	6	
	Monomers				Monon	ners	

Figure 4: Tangent-tangent correlation functions for chain backbone of (a) PS and (b) $P\alpha MS$.

dynamics, also does not give the right persistence length.³² Hence we developed new potential parameters for the alkyl chain backbone of PS and P2VP (Table 1), plotted in Figure 3. These values were obtained by starting with the potential of Ref. 32 and performing NPT simulations, and modifying the potential to obtain a persistence length for PS and P2VP chains close to experiment.

In simulations, we measure the persistence length from tangent-tangent correlation functions along the backbone $\langle t_0 \cdot t_n \rangle$ (Figure 4). The persistence length is the length of backbone over which the tangent correlations fall by a factor of 1/e. For PS and P2VP, with our adjusted potentials we find the persistence length to be around 2.85 monomers, in reasonable agreement with experimental values ranging from 3 to 5 monomers. ³³ Getting the right stiffness matters because it affects how chains pack in the system and how easily other chain segments come near, which can significantly affect χ .

The PS-P2VP morphing simulations consisted of 200 chains of 10 monomers each. The simulations were performed at 500 K and 1 bar for 30 ns.

The dielectric constant ϵ_r quantifies the electrostatic screening brought about by a ma-

terial. MD simulations typically set the background dielectric constant at $\epsilon=1$. Indeed, TRAPPE potential parameters for PS and P2VP were developed with $\epsilon=1$. However for typical hydrocarbon liquids, the "electronic" contribution to ϵ is usually around 2. The pyridine ring in P2VP, has a large dipole moment of around 2.2 D.³⁴ Hence the value of background dielectric constant used in the simulations may be important for evaluating χ for the mixture. To explore this, we perform morphing simulations for PS/P2VP using $\epsilon=1$ and $\epsilon=2$.

PI /SPI

To morph PI chains to sPI chains, we transform double bonds in the chain to single bonds. LJ interaction parameters of the atoms involved in the double bond and bonded interactions involving the double bond are likewise modified. The system consists of 800 chains of 10 monomers each. Because we compare to experimental results which contain predominately cis-PI, we build our chains all cis accordingly. Hence our melts start with all cis configurations for PI. We simulate for 200 ns with a time step of 2 fs at 500 K and 1 bar. The longer simulation runtime is necessary, because are trying to accurately determine a small χ .

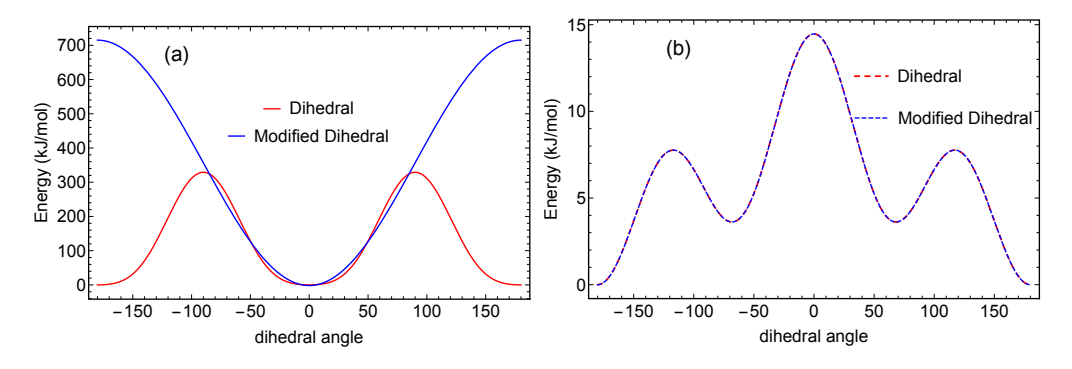


Figure 5: Dihedral potential acting on PI across the double bond at (a) $\lambda = 0$ and (b) $\lambda = 1$. Red and blue curves represent original and modified dihedral potentials, respectively.

Morphing the dihedral potential applied across the double bond requires a special modification. The dihedral potential across the double bond for PI and corresponding dihedral in sPI are represented by red curves in Figure 5 (a) and (b). While morphing from PI to

sPI, the energy barrier between cis (dihedral angle = 0°) and trans (dihedral angle = 180°) decreases. Eventually, the energy barrier is small enough for chains to switch between trans and cis. But the corresponding equilibration time is awkwardly long.

To circumvent this problem, we modify the dihedral function for PI as shown by the blue curve in Figure 5 (a). This modification has no effect on the distribution of dihedrals in PI, but we avoid the configuration switch between *cis* and *trans* states. The initial and final states for the morphing process remain the same, we modify only the path of morphing dihedrals to favor rapid equilibration.

$PS/P\alpha MS$

We start with a pure melt of $P\alpha MS$ and morph a bead representing a terminal methyl (CH₃) group on every monomer into nothing. We accomplish this by systematically decreasing the LJ interaction parameters of the methyl beads to zero. In general, when atoms are being "deleted" in this way, some may overlap with other vanishing atoms as the repulsive LJ interactions become smaller. Here, only a small percentage (8.3 percent) of atoms vanish, and we observe no anomalies resulting from vanishing atoms coming too close.

Our PS/P α MS system consist of 200 chains of 10 monomers. Because χ is quite small for the system, we perform long simulations spanning over 800 ns and a time step of 2 fs at 300 K and 1 bar pressure.

To match the experimental persistence length of P α MS, we again modify the dihedral potential starting from Zhou et al. as described above. (see Figure 4 (b)). The simulated α MS chains have a persistence length of 2.7 monomers, consistent with experimental values ranging from 2.5 to 4.³³ The dihedral potential parameters are listed in Table 1, and the dihedral potential is plotted in Figure 3.

Results

PE/PEO

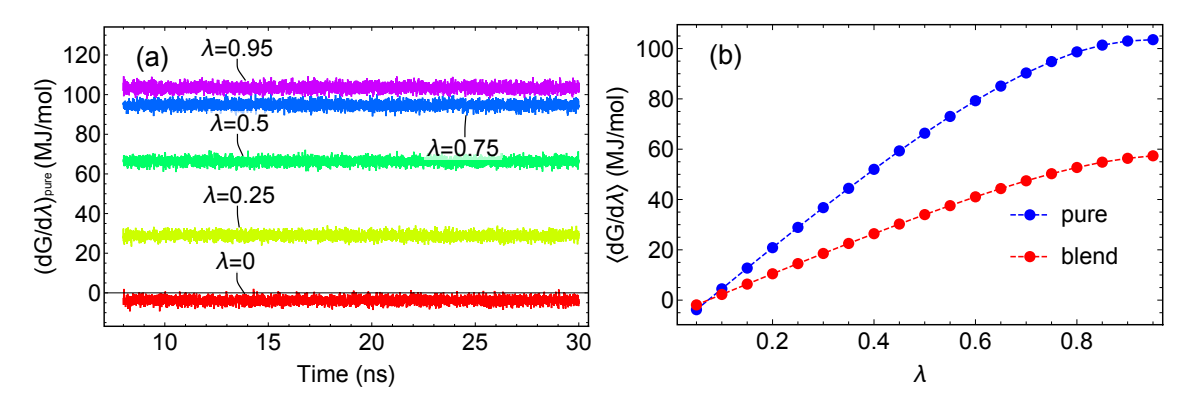


Figure 6: Free energy integrand $\langle dG/d\lambda \rangle$ versus λ for PE/PEO: (a) Time series of $dG/d\lambda$ for morphing from PE to PEO at various λ s. (b) $\langle dG/d\lambda \rangle$ versus λ for pure (PE to PEO) and blend PE to PE/PEO) system. Error bars are too small to be seen in the plot.

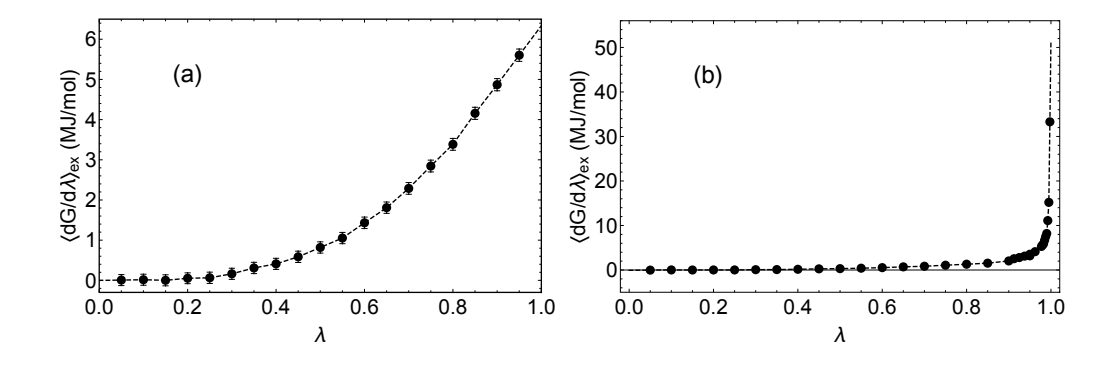


Figure 7: Excess free energy integrand $\langle dG/d\lambda \rangle_{ex}$ versus λ for PE/PEO at T = 500 K from (a) united atom morphing simulations and (b) all-atom morphing simulations. Error bars are too small to be seen in the plot for all-atom simulations.

We measure the free energy integrand $\langle dG/d\lambda \rangle$ at different λ values using the morphing simulations using equation 3. In the morphing simulation series, all and half of PE chains in the system are morphed to PEO to obtain pure PEO and a PE/PEO blend respectively. As seen in Figure 6 (a), $dG/d\lambda$ fluctuates about an average value throughout the time series. The autocorrelation time τ for the integrand is 4 ps; we compute the statistical error on $\langle dG/d\lambda \rangle$, defined as the standard deviation for $dG/d\lambda$ time series divided by the square root

of the number of uncorrelated values. The error bars are too small to be seen in the plot.

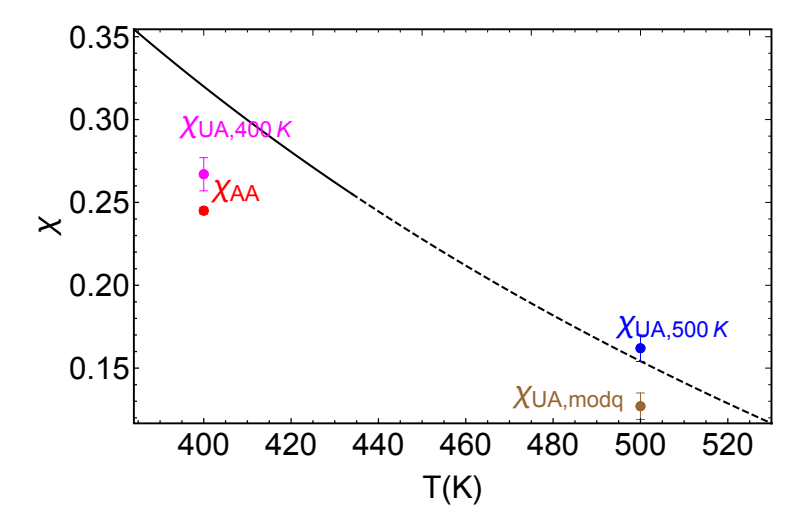


Figure 8: Flory Huggins interaction parameter χ for PE/PEO from united atom simulations (χ_{UA} , blue) and all-atom simulations (χ_{UA} , red); Black solid line represents χ from experiments in the valid temperature range and black dotted line is extrapolation to simulation conditions.³³ Error bar for atomistic simulation χ is smaller than the marker.

The excess free energy integrand as a function of λ is determined using eqn 1 (Figure 7 (a)). The positive area under the excess curve implies that the system pays a free energy cost to mix these chains. We numerically integrate $\langle dG/d\lambda \rangle_{ex}$ with respect to λ to compute χ for PE/PEO (Equation 2), which amounts to 0.169 \pm 0.008 (Figure 8).

The errors on $\langle dG/d\lambda \rangle_{\lambda}$, $(\delta \langle dG/d\lambda \rangle_{\lambda})$, are propagated to the free energy of morphing G as given by

$$\delta G = \left(\sum_{\lambda} (\delta \langle dG/d\lambda \rangle_{\lambda} \Delta \lambda)^{2}\right)^{0.5} \tag{5}$$

We use equation 5 to calculate the uncertainty of G_{AB} and G_{B} . The error of ΔG_{ex} is computed by adding the squares of errors on G_{AB} and ϕ_{B} times G_{B} and taking the square root of the sum. The uncertainty of ΔG_{ex} is propagated to χ as per equation 2 in the paper.

 χ from united atom simulations for PE/PEO blend agrees with experimental measurements extrapolated to simulation conditions. Experimental values for χ of all the polymer blends studied in this paper were obtained from Eitouni et al., which has a collection of reliable data for χ of different polymer blends.³³ For PE/PEO, the experimental χ was obtained

from Almdal et al. 35

For comparison, we determined χ for PE/PEO using all-atom (AA) morphing simulations (Figure 8). The excess free energy integrand versus λ for all-atom simulations steeply increases as λ approaches 1, so additional simulations were required to define the curve accurately (Figure 7 (b)). χ obtained from atomistic simulations is 0.245 \pm 0.002, significantly lower than the experimental value at 400 K. UA morphing simulations of PE/PEO with short chains and T = 400 K predict a χ = 0.267 \pm 0.01, closer to the experimental value.

UA MD simulation results for χ fare better with experiments compared to AA simulations. We compare the density of PE melt in all-atom and UA MD simulations with experimental values. We find that the UA force-field model emulated physical properties for PE melt better than the AA force-field model for different chain lengths of PE. The difference in agreement with experiments is because of the differences in the potential parameters used to represent the interactions within the system. The results highlight that using the right potential parameters is important to obtain reliable results for χ .

When comparing morphing simulations of PE/PEO with TRAPPE potential parameters with that of modified TRAPPE potential parameters ($\chi_{UA,500K}$ vs $\chi_{UA,modq}$ respectively) we find that $\chi_{UA,modq}$ is lower than $\chi_{UA,500K}$. This can be rationalized by decrease in disparity between coulombic interactions resulting from PE and PEO, bringing down the energy cost to mix these two polymers. $\chi_{UA,500K}$ is closer to the experimental χ value for PE/PEO and hence, we use results from morphing simulations with original TRAPPE potential parameters further along the paper.

PS/P2VP

We determine the excess free energy integrand $\langle dG/d\lambda \rangle_{ex}$ as a function of λ for PS/P2VP from morphing simulations (Figure 9). χ for PS/P2VP was determined with two material dielectric constants, $\epsilon = 1$ and $\epsilon = 2$ employed in MD simulations. Predicted χ for PS/P2VP amounts to 0.139 ± 0.002 with a background dielectric constant $\epsilon = 1$ and 0.050 ± 0.001 for

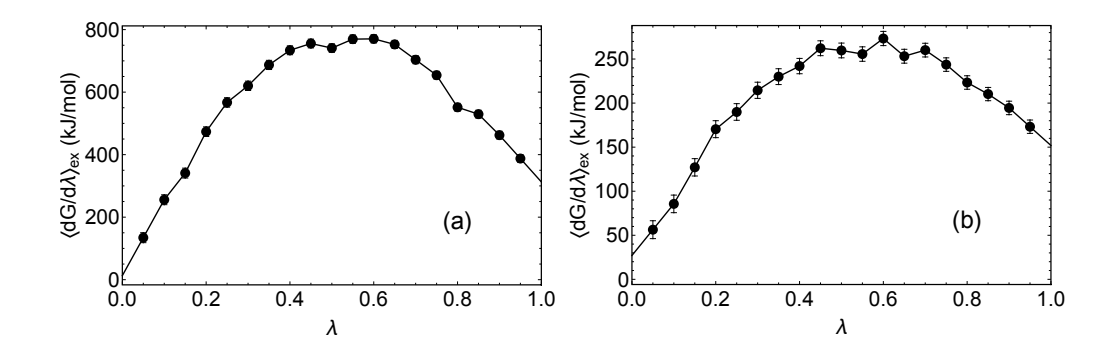


Figure 9: Excess free energy integrand $\langle dG/d\lambda \rangle_{ex}$ versus λ for PS/P2VP at T = 500 K with background dielectric constant (a) $\epsilon = 1$ and (b) $\epsilon = 2$.

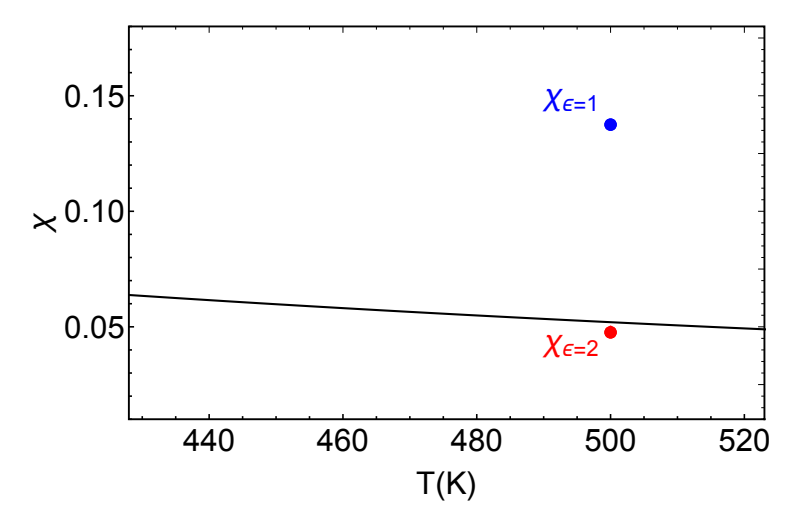


Figure 10: Flory Huggins interaction parameter χ for PS/P2VP for background dielectric constant $\epsilon=1$ (blue) and $\epsilon=2$ (red); Black solid line represents χ from experiments in the valid temperature range and black dotted line is extrapolation to simulation conditions. ³³

 $\epsilon = 2$. We find that our predicted χ when $\epsilon = 2$ fares better when compared to experimental values, despite the fact that the TRAPPE potential parameters for PS and P2VP were developed using $\epsilon = 1$.³³ This comparison highlights the fact that the results are sensitive to force field parameters used in the simulations.

PI/sPI

We compute the excess free energy integrand $\langle dG/d\lambda \rangle_{ex}$ versus λ for PI/sPI using eqn 2 from morphing simulations. Since χ is of the order 10^{-3} , we use simulation trajectories spanning 200 ns for each value of λ , to obtain reliable values for the excess free energy integrand. We

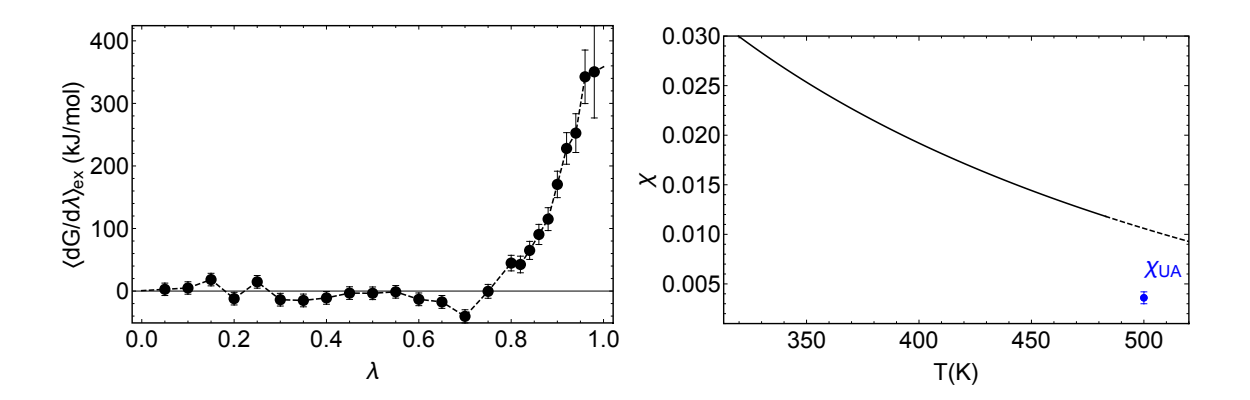


Figure 11: (a) Excess free energy integrand $\langle dG/d\lambda \rangle_{ex}$ versus λ for PI/sPI at T = 500 K; (b) Flory Huggins interaction parameter χ (blue) for PI/sPI; Black solid line represents χ from experiments in the valid temperature range and black dotted line is extrapolation to simulation conditions.³³

determine χ to be 0.004 \pm 0.001 for PI/sPI from simulations. The χ predicted for PI/sPI is in rough agreement with experimental measurements of χ^{33} (Figure 11 b).

$PS/P\alpha MS$

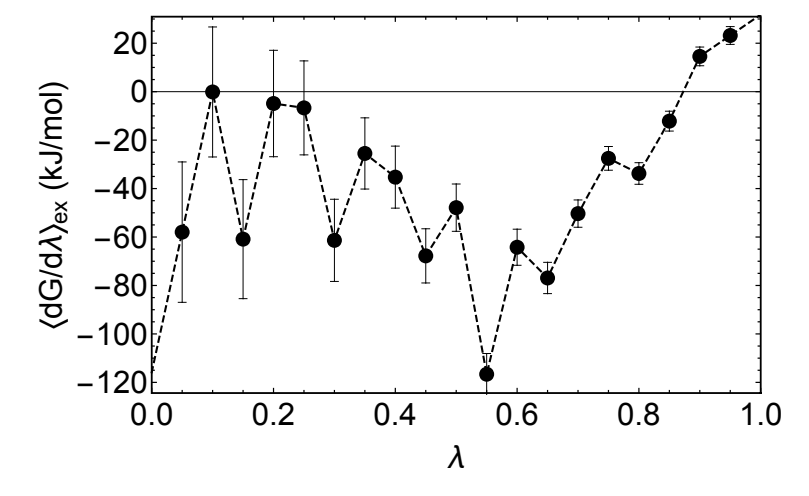


Figure 12: Excess free energy integrand $\langle dG/d\lambda \rangle_{ex}$ versus λ for PS/P α MS at T = 500 K.

The excess free energy integrand $\langle dG/d\lambda \rangle_{ex}$ versus λ from morphing simulations for PS/P α MS is shown in Figure 12. For each λ , we analyze simulation trajectories spanning over 800 ns. Despite such long simulations, we do not obtain a smooth curve for the excess free energy integrand. Also, the area under the curve is slightly negative, whereas the

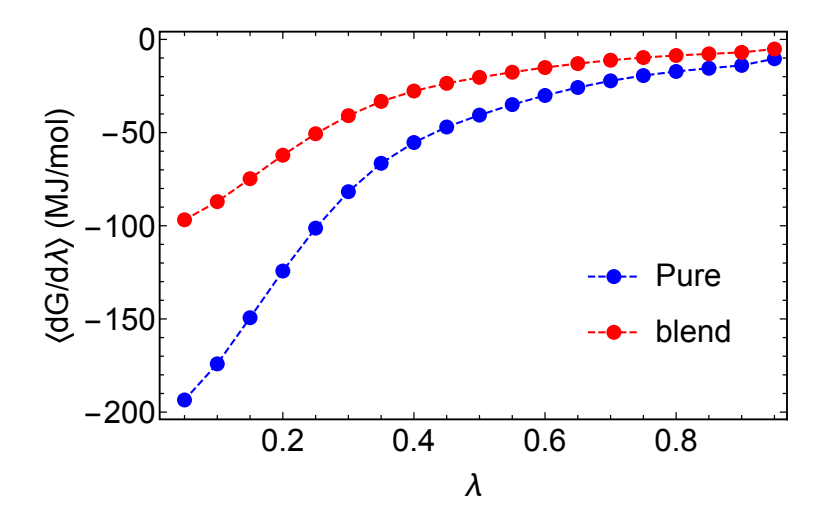


Figure 13: Free energy integrand $\langle dG/d\lambda \rangle$ versus λ for PS/P α MS at T = 500 K for pure (PS) (blue) and blend (PS/P α MS) (red) systems.

experimental value for χ of PS/P α MS is small and positive. The experimental value of χ of PS/P α MS extrapolated to simulation conditions is 0.0026.³³

The free energy integrands from PS/P α MS morphing simulations (Figure 13) range in tens of megajoules (MJ), whereas their differences as given by eq 2 and range in tens of kilojoules (kJ). As such, we are finding a small difference between two relatively large quantities. The morphing method approaches its limit for such small values of χ .

Energetic and entropic contributions to χ

The excess Gibbs free energy of mixing can be written as

$$\Delta G_{ex} = \Delta E_{ex} - T \Delta S_{ex} + P \Delta V_{ex} \tag{6}$$

Correspondingly, we have three contributions to χ :

$$\chi = \chi_E + \chi_S + \chi_V \tag{7}$$

We can separately measure the energetic and volumetric contributions χ_E and χ_V in morphing simulations. We measure the change in system energy on morphing for pure and

blend systems, their difference weighted by mole fraction of species gives χ_E . Similarly, system volume changes upon morphing give the volumetric contribution to χ . We have tabulated χ_E for the first three systems in Table 2. χ_V is essentially zero for all the systems. The entropic contribution χ_S is calculated using eq. 7.

Table 2: Flory Huggins interaction parameter χ and energetic part χ_E for different systems. χ_V is nearly zero for all the cases.

Blend	χ	χ_E	χ_S
PE/PEO	0.1693 ± 0.0080	0.4741	-0.3048
$PS/P2VP (\epsilon_r = 1)$	0.1375 ± 0.0015	0.2090	-0.0715
$PS/P2VP (\epsilon_r = 2)$	0.0476 ± 0.0016	0.0995	-0.0519
PI/sPI	0.0036 ± 0.0006	0.0010	0.0026

For PE/PEO and PS/P2VP, there is a sizable negative entropic contribution to χ . This implies that the blends have greater configurational freedom compared to the respective pure melts. We hypothesize that interactions between dipoles on PEO or P2VP chains lead to local correlations, which decrease configurational freedom and hence reduce the entropy. More dipole-dipole interactions are found in pure melts, because the concentration of dipoles is higher.

We support this idea by measuring the dipole-dipole interaction energy between near neighbor dipoles in the blends and pure melts. Analyzing molecular dipoles in the simulation trajectories, we find that dipole-dipole interactions between PEO molecules are significant compared to thermal fluctuations. Hence local configurations are expected to be affected by dipole-dipole interactions. This holds for interactions between dipoles on P2VP chains as well. As a consequence, we have a net negative entropic contribution to χ for PS/P2VP and PEO/PE. (See Appendix A for further details.)

In contrast, for PI/sPI, more than 70 percent of the *positive* contribution to χ is entropic. Chemically, PI and sPI have very similar molecular structures, which lead to very similar cohesive energy densities in the pure melts or the blend. But their backbone persistence lengths are different so that chains are expected to pack differently in the pure melt versus the blend.²⁵ Hence most of the demixing tendencies in PI/sPI are caused by a change in

packing entropy between the pure melts and the blend.

Conclusions

We combine united atom MD simulations and thermodynamic integration along the path of transformation of chains to determine χ for real polymer blends. Previously, the morphing method was used to study effect of different factors on χ using simple bead-spring chains. In this study, we predict χ for real polymer blends, employing different morphing schemes including modifying LJ parameters and partial charges, changing double bonds to single bonds, and deletion of atoms.

For PE/PEO, predicted values for χ are in agreement with experimental measurements extended to simulation conditions. χ obtained using all-atom morphing simulations is considerably lower than the experimental value, indicating the importance of the potential parameters used in morphing simulations. Also, for reasons of simulation efficiency, very short chains were used in atomistic simulations, which may affect how chains pack in the melt.

For PS/P2VP, results for χ depend significantly on the value of background dielectric constant used; χ obtained using a typical "electronic" dielectric constant of $\epsilon = 2$ agrees well with experimental χ for PS/P2VP. From these two examples, we infer that choosing the right potential parameters is essential to obtain good values for χ .

Morphing simulations for PI/sPI predict a value for χ that agrees reasonably with experiments. But for PS/P α MS, we are not able to obtain a meaningful χ value; computing a small excess free energy quantity as the difference between two large quantities gives big relative errors for a small χ . For PS/P α MS, we reach the limits of the morphing method.

Using morphing simulations, we can predict how different factors affect mixing of blends. When ϵ is varied in the simulations, the absolute value for χ , χ_E , and χ_S also vary. Partial charges present in atoms interact differently within different dielectric environments, changing how much enthalpy and entropy contribute to blend χ .

For PE/PEO and PS/P2VP, there is a negative χ contribution resulting from lesser restrictions from dipole-dipole interactions on chain configurations in the blend compared to the pure melts. For PI/sPI, a positive entropic contribution to χ is caused by differences in local packing for chains of similar cohesive energy difference but different stiffness.

To conclude the discussion, we identify the limitation of the morphing method. To determine χ using this method, the components of the blend need to be structurally related. The transformation of polymers during the simulation series involves modifying the parameters defining different interactions within the system. For a structurally unrelated system, multiple atoms might be altered, added, or deleted. For such transformation, tracking all the parameters that needed to be varied might be a daunting task and not worth the effort.

Appendix A

The negative entropic contribution to χ for PE/PEO and PS/P2VP implies that more local conformational freedom is available for blends than pure melts, beyond that accounted for by ideal translational entropy. We attribute this effect to dipoles present in these systems; interactions between dipoles may cause alignment of moieties bearing dipoles. The resulting correlations between nearby dipoles reduce the entropy. Because more dipole-dipole interactions are present in pure melts of PEO and P2VP, the entropy reduction is more significant in pure melts compared to blends, so these interactions negatively contribute to χ . If dipole-dipole interactions are significant compared to thermal fluctuations, negative contributions to χ will also be significant.

Reduction in orientational entropy for a dipole in potential field U relative to a freely rotating dipole can be written perturbatively as

$$\Delta S/k = -(1/2)\beta^2 \langle U^2 \rangle \tag{8}$$

Here U is the dipole-dipole interaction potential given by

$$U = \frac{3(p_1 \cdot n)(p_2 \cdot n) - p_1 \cdot p_2}{4\pi\epsilon_0 r} \tag{9}$$

The brackets $\langle ... \rangle$ denotes the unbiased average over orientations of dipole p_2 with respect to p_1 and the direction of normal between p_1 and p_2 , with fixed distance r between the dipoles. (Equation 8 is obtained perturbatively from the information theoretic formula $S/k = -\sum_r P_r \log P_r$, where P_r is proportional to the Boltzmann factor $e^{-\beta U}$, and βU is assumed small.)

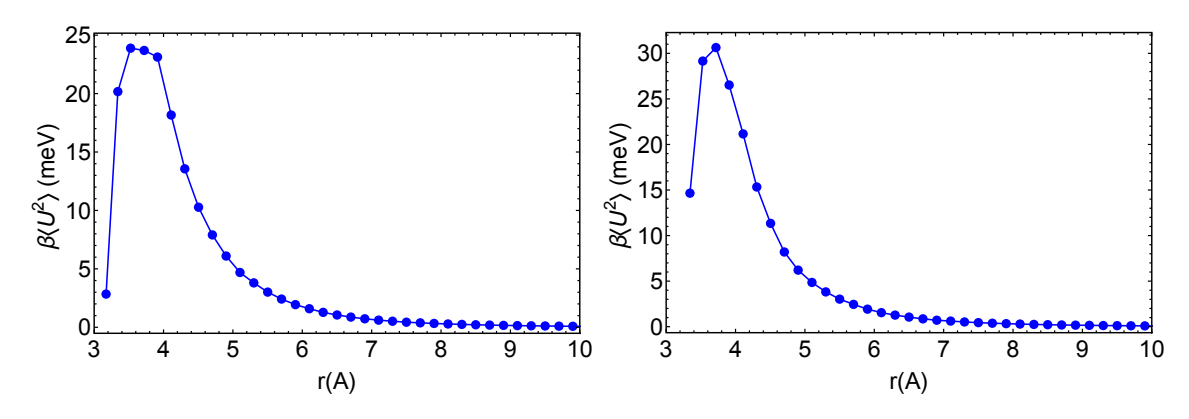


Figure 14: Reduction in orientational entropy for pairs of PEO dipoles at separation r in (a) PEO melt and (b) PE/PEO.

For PE/PEO, using equation 8, we estimate the orientational entropy reduction for PEO molecules in pure PEO melts and PE/PEO blends in simulations. From Figure 14, we see that near-neighbor dipole-dipole interactions in PEO melts and PEO/PE blends are comparable with thermal energy fluctuations (kT) (43 meV at 500 K). Hence dipole-dipole interactions are large enough to affect chain orientations for PE/PEO (as well as PS/P2VP), and these entropic interactions contribute negatively to χ .

Acknowledgement

Financial support from the National Science Foundation under awards DMREF-1629006 and DMREF-1921854 are acknowledged.

References

- (1) Stoelting, J.; Karasz, F. E.; Macknight, W. J. Dynamic mechanical properties of poly(2,6-dimethyl-1,4-phenylene ether)-polystyrene blends. *Polymer Engineering & Science* 1970, 10, 133–138, DOI: https://doi.org/10.1002/pen.760100302.
- (2) Aid, S.; Eddhahak, A.; Khelladi, S.; Ortega, Z.; Chaabani, S.; Tcharkhtchi, A. On the miscibility of PVDF/PMMA polymer blends: Thermodynamics, experimental and numerical investigations. *Polymer Testing* 2019, 73, 222-231, DOI: https://doi.org/10.1016/j.polymertesting.2018.11.036.
- (3) Macosko, C. W. Morphology development and control immiscible polymer blends. MacromolecularSymposia 2000, 149, 171-184, DOI: https://doi.org/10.1002/1521-3900(200001)149:1<171::AID-MASY171>3.0.CO;2-8.
- (4) Shaw, M. T. Processing and commercial application of polymer blends. *Polymer Engineering & Science* **1982**, *22*, 115–123, DOI: 10.1002/pen.760220212.
- (5) Bates, F. S.; Fredrickson, G. H. Block copolymer thermodynamics: theory and experiment. *Annual Review of Physical Chemistry* **1990**, *41*, 525–557.
- (6) Bates, C. M.; Bates, F. S. 50th Anniversary Perspective: Block PolymersPure Potential.

 *Macromolecules** 2017, 50, 3–22, DOI: 10.1021/acs.macromol.6b02355.
- (7) Robeson, L. M. Applications of polymer blends: Emphasis on recent advances. *Polymer Engineering & Science* **1984**, *24*, 587–597, DOI: 10.1002/pen.760240810.

- (8) Tao, Y.; McCulloch, B.; Kim, S.; Segalman, R. A. The relationship between morphology and performance of donor-acceptor rod-coil block copolymer solar cells. *Soft Matter* **2009**, *5*, 4219–4230, DOI: 10.1039/B907836C.
- (9) Guo, C.; Lin, Y.-H.; Witman, M. D.; Smith, K. A.; Wang, C.; Hexemer, A.; Strzalka, J.; Gomez, E. D.; Verduzco, R. Conjugated Block Copolymer Photovoltaics with near 3% Efficiency through Microphase Separation. *Nano Letters* 2013, 13, 2957–2963, DOI: 10.1021/nl401420s, PMID: 23687903.
- (10) Rubinstein, M.; Colby, R. H. *Polymer Physics*; Oxford: Oxford University Press, 2003.
- (11) Nishi, T.; Wang, T. T. Melting Point Depression and Kinetic Effects of Cooling on Crystallization in Poly(vinylidene fluoride)-Poly(methyl methacrylate) Mixtures. *Macromolecules* 1975, 8, 909–915, DOI: 10.1021/ma60048a040.
- (12) Barlow, J. W.; Paul, D. R. The importance of enthalpic interactions in polymeric systems. *Polymer Engineering & Science* **1987**, *27*, 1482–1494, DOI: https://doi.org/10.1002/pen.760272003.
- (13) Kim, C.; Paul, D. Interaction parameters for blends containing polycarbonates: 1. Tetramethyl bisphenol-A polycarbonate/polystyrene. *Polymer* 1992, 33, 1630–1639, DOI: https://doi.org/10.1016/0032-3861(92)91059-B.
- (14) Shiomi, T.; Kohno, K.; Yoneda, K.; Tomita, T.; Miya, M.; Imai, K. Thermodynamic interactions in the poly(vinyl methyl ether)-polystyrene system. *Macromolecules* 1985, 18, 414–419, DOI: 10.1021/ma00145a020.
- (15) Olabisi, O. Polymer Compatibility by Gas-Liquid Chromatography. *Macromolecules* 1975, 8, 316–322, DOI: 10.1021/ma60045a014.
- (16) Leibler, L. Theory of Microphase Separation in Block Copolymers. Macromolecules 1980, 13, 1602–1617, DOI: 10.1021/ma60078a047.

- (17) Fredrickson, G. H.; Liu, A. J.; Bates, F. S. Entropic corrections to the Flory-Huggins theory of polymer blends: Architectural and conformational effects. *Macromolecules* 1994, 2503 2511.
- (18) Russell, T. X-ray and neutron reflectivity for the investigation of polymers. *Materials Science Reports* **1990**, *5*, 171 271, DOI: 10.1016/S0920-2307(05)80002-7.
- (19) Helfand, E.; Tagami, Y. Theory of the interface between immiscible polymers. *Journal of Polymer Science Part B: Polymer Letters* **1971**, *9*, 741–746.
- (20) Tambasco, M.; Lipson, J. E. G.; Higgins, J. S. Blend Miscibility and the Flory-Huggins Interaction Parameter: A Critical Examination. *Macromolecules* 2006, 39, 4860–4868, DOI: 10.1021/ma060304r.
- (21) Groot, R. D.; Warren, P. B. Dissipative particle dynamics: Bridging the gap between atomistic and mesoscopic simulation. *The Journal of Chemical Physics* **1997**, *107*, 4423–4435, DOI: 10.1063/1.474784.
- (22) Chremos, A.; Nikoubashman, A.; Panagiotopoulos, A. Z. Flory-Huggins parameter χ, from binary mixtures of Lennard-Jones particles to block copolymer melts. The Journal of Chemical Physics 2014, 140, 054909, DOI: 10.1063/1.4863331.
- (23) Callaway, C. P.; Hendrickson, K.; Bond, N.; Lee, S. M.; Sood, P.; Jang, S. S. Molecular Modeling Approach to Determine the Flory-Huggins Interaction Parameter for Polymer Miscibility Analysis. *ChemPhysChem* 19, 1655–1664, DOI: https://doi.org/10.1002/cphc.201701337.
- (24) Chen, Q. P.; Chu, J. D.; DeJaco, R. F.; Lodge, T. P.; Siepmann, J. I. Molecular Simulation of Olefin Oligomer Blend Phase Behavior. *Macromolecules* **2016**, *49*, 3975–3985, DOI: 10.1021/acs.macromol.6b00394.

- (25) Kozuch, D.; Zhang, W.; Milner, S. Predicting the Flory-Huggins χ Parameter for Polymers with Stiffness Mismatch from Molecular Dynamics Simulations. *Polymers* 2016, 8, 241, DOI: 10.3390/polym8060241.
- (26) Zhang, W.; Gomez, E. D.; Milner, S. T. Predicting Flory-Huggins χ from Simulations. Phys. Rev. Lett. 2017, 119, 017801, DOI: 10.1103/PhysRevLett.119.017801.
- (27) Shetty, S.; Adams, M. M.; Gomez, E. D.; Milner, S. T. Morphing Simulations Reveal Architecture Effects on Polymer Miscibility. *Macromolecules* **2020**, *53*, 9386–9396.
- (28) Collin D Wick,; John M Stubbs,; Neeraj Rai,; ; J Ilja Siepmann, Transferable Potentials for Phase Equilibria. 7. Primary, Secondary, and Tertiary Amines, Nitroalkanes and Nitrobenzene, Nitriles, Amides, Pyridine, and Pyrimidine. 2005,
- (29) Collin D Wick,; Marcus G Martin,; ; J Ilja Siepmann, Transferable Potentials for Phase Equilibria. 4. United-Atom Description of Linear and Branched Alkenes and Alkylbenzenes. **2000**,
- (30) Hess, B.; Kutzner, C.; van der Spoel, D.; Lindahl, E. GROMACS 4: Algorithms for Highly Efficient, Load-Balanced, and Scalable Molecular Simulation. *Journal of Chemical Theory and Computation* **2008**, *4*, 435–447.
- (31) Inc., W. R. Mathematica, Version 12.2. https://www.wolfram.com/mathematica, Champaign, IL, 2020.
 - () Chen, Q. P.; Xie, S.; Foudazi, R.; Lodge, T. P.; Siepmann, J. I. Understanding the Molecular Weight Dependence of and the Effect of Dispersity on Polymer Blend Phase Diagrams. *Macromolecules* **2018**, *51*, 3774–3787, DOI: 10.1021/acs.macromol.8b00604.
- (32) Zhou, Y.; Milner, S. T. Short-Time Dynamics Reveals Tg Suppression in Simulated Polystyrene Thin Films. *Macromolecules* **2017**, *50*, 5599–5610.

- (33) Eitouni, H. B.; Balsara, N. P. In *Physical Properties of Polymers Handbook*; Mark, J. E., Ed.; Springer, New York, NY: New York, NY, 2007; pp 339–356.
- (34) Headen, T. F.; Cullen, P. L.; Patel, R.; Taylor, A.; Skipper, N. T. The structures of liquid pyridine and naphthalene: the effects of heteroatoms and core size on aromatic interactions. *Phys. Chem. Chem. Phys.* **2018**, *20*, 2704–2715, DOI: 10.1039/C7CP06689A.
- (35) Almdal, K.; Hillmyer, M. A.; Bates, F. S. Influence of Conformational Asymmetry on Polymer – Polymer Interactions: An Entropic or Enthalpic Effect. *Macromolecules* 2002, DOI: 10.1021/ma020148y.

Graphical TOC Entry

